Howard Hughes Medical Institute

Published as: *Clin Cancer Res*. 2017 September 15; 23(18): 5622–5630.

# Age and gender associations of virus positivity in Merkel cell carcinoma characterized using a novel RNA *in situ* hybridization assay

**Lisha Wang**[1,*], **Paul W. Harms**[1,2,3,*], **Nallasivam Palanisamy**[1,2,4], **Shannon Carskadon**[4], **Xuhong Cao**[1,5], **Javed Siddiqui**[1,2], **Rajiv M. Patel**[2,3], **Sylvia Zelenka-Wang**[1], **Alison B. Durham**[3,6], **Douglas R. Fullen**[2,3], **Kelly L. Harms**[3,6], **Fengyun Su**[1], **Sudhanshu Shukla**[1], **Rohit Mehra**[1,2,6], and **Arul M. Chinnaiyan**

[1]Michigan Center for Translational Pathology, University of Michigan Health System, Ann Arbor, MI 48109, USA

[2]Department of Pathology, University of Michigan Health System, Ann Arbor, MI 48109, USA

[3]Department of Dermatology, University of Michigan Health System, Ann Arbor, MI 48109, USA

[4]Department of Urology, Henry Ford Health System, Detroit, MI 48202, USA

[5]Howard Hughes Medical Institute, Ann Arbor, MI 48109, USA

[6]Comprehensive Cancer Center, University of Michigan Health System, Ann Arbor, MI 48109, USA

[7]Department of Urology, University of Michigan Health System, Ann Arbor, MI 48109, USA

## Abstract

**Purpose—**Merkel cell carcinoma (MCC) is a highly aggressive neuroendocrine tumor of the skin. Merkel cell polyomavirus (MCPyV) plays an oncogenic role in the majority of MCCs. Detection of MCPyV in MCCs has diagnostic utility and prognostic potential. We investigated whether RNAscope, an RNA *in situ* hybridization (ISH) assay for detection of RNA transcripts in tissues, is useful for MCPyV detection.

**Experimental Design—**We applied an RNAscope probe targeting MCPyV T antigen transcripts on tissue microarrays (TMAs) and whole tissue sections encompassing 87 MCCs from 75 patients, 14 carcinomas of other types, and benign tissues. For comparison, quantitative PCR (qPCR) was performed on 57 cases of MCC from 52 patients.

**Results—**RNA-ISH demonstrated the presence of MCPyV in 37/75 (49.3%) cases. Notably, tumors from younger patients (< 73 years) had a significantly higher virus positivity than those from elderly patients (≥ 73 years) (64.9% vs. 34.2%, $P$=0.011). Female patients had a higher positive rate of MCPyV than male patients (66.7% vs. 39.6%, $P$=0.032). Data from both RNA-ISH and qPCR were available for 57 samples. Considering MCPyV qPCR as the gold standard for

[†]**Corresponding Author:** Arul M. Chinnaiyan, Michigan Center for Translational Pathology, Comprehensive Cancer Center, 1400 E. Medical Center Drive, Ann Arbor, MI 48109, USA. Tel. +1 734 6154062; Fax: +1 734 6154498.

[*]These authors contributed equally to this work.

determining MCPyV status, RNAscope had 100% sensitivity and 100% specificity. There was a strong correlation between qPCR copy number and RNA-ISH product score (Spearman's correlation coefficient $R^2 = 0.932$, $P < 0.0001$).

**Conclusions—**RNA-ISH is comparably sensitive to qPCR for detection of MCPyV and allows for correlation with tissue morphology. This study also reveals a significant association between age, gender, and MCPyV positivity.

### Keywords

Merkel cell polyomavirus; Merkel cell carcinoma; RNA *in situ* hybridization

## Introduction

Merkel cell carcinoma (MCC) is an aggressive neuroendocrine carcinoma associated with high rates of metastasis and mortality. MCC predominantly arises in elderly and immunosuppressed patients. Although rare, the incidence of MCC has nearly tripled in incidence over the past 20 years (1, 2).

A major breakthrough in the understanding of MCC pathogenesis came with the discovery of Merkel cell polyomavirus (MCPyV) via digital transcriptome analysis (3). MCPyV is a DNA virus that likely mediates tumorigenesis via large T antigen (LTAg) binding to the tumor suppressor RB1 and small T antigen (sTAg) upregulation of oncoprotein stability and mTOR activation (1, 2). Unlike MCPyV-positive tumors, MCPyV-negative MCC tumors display high mutation burdens, *TP53* and *RB1* mutations, and UV-signature mutational profiles, suggesting a molecular dichotomy between MCPyV-positive and MCPyV-negative tumors that may have translational relevance (4–7).

MCPyV is detected in a majority of MCC tumors in most patient populations, although there may be lower incidence in some regions (2, 3, 8). Thus far, MCC appears to be the only tumor type to harbor MCPyV with significant frequency. Hence, the presence of MCPyV is emerging as a marker to aid in distinction of MCC from morphologically-similar tumors, such as non-cutaneous small cell carcinoma (9–13). The most common assays for detection of MCPyV are quantitative PCR (qPCR) and immunohistochemistry (IHC). qPCR is considered the most sensitive assay in common use for detection of MCPyV, but it has several limitations. Evaluation of multiple amplicons is necessary for maximal sensitivity, as neither LTAg nor sTAg detection alone is fully sensitive (14). In addition, low MCPyV qPCR signal may be detected due to infection by wild-type virus in normal tissues (15), and qPCR does not allow for direct correlation with morphology to confirm that the signal is originating in tumor cells. IHC allows for correlation with tissue morphology. The most commonly used antibody is CM2B4, which specifically detects MCPyV LTAg and not other polyomavirus T-antigens (9–13). Multiple reports have found IHC with CM2B4 antibody to be less sensitive than qPCR (14, 16, 17). Existing assays have limitations for routine clinical practice, warranting the need for development of new MCPyV detection methods.

Advances in RNA *in situ* hybridization (ISH) have revolutionized the ability to assess RNA expression in multiple specimen types, including formalin-fixed paraffin-embedded (FFPE)

tissues (18, 19). RNAscope technology provides single-molecule sensitivity and resolution, enabling quantification of specific RNA molecules at the single cell level (20). Recent development of proprietary RNAscope probes complementary to MCPyV LTAg/sTAg mRNA permits direct visualization of viral transcripts with spatial and morphological context. The purpose of this study was to compare the RNAscope approach for MCPyV detection with qPCR, thereby providing an alternative, sensitive assay with which to identify this important marker. Association of MCPyV status, determined by RNAscope, with clinicopathological features of MCC patients was further assessed.

## Materials and Methods

### MCC cohort

This study was approved by the University of Michigan Hospital System Institutional Review Board (IRB Study ID: HUM0045834) and were conducted in accordance with the United Stated Common Rule; archival formalin-fixed, paraffin-embedded tissues collected for diagnostic purposes were used according to waiver of consent protocol approved by the institutional review board. As per standard protocol at our institution, diagnostic material for all MCC cases underwent review by a board-certified dermatopathologist, followed by clinical case review in a multidisciplinary tumor board. Cases were re-reviewed by the study pathologist for further diagnostic confirmation. This cohort consisted of 87 tumors from 75 unique patients presented on whole tissue sections and three previously constructed tissue microarrays (TMA), including two TMAs with 0.8 mm cores in duplicate and one TMA with 0.6 mm cores in triplicate. These TMAs also included tissues from four non-cutaneous small cell carcinomas, nine cervical carcinomas, six benign cervix, and one basal cell carcinoma. For normal skin tissue samples, FFPE blocks were selected that contained non-lesional skin from surgical excisions performed on the forehead and scalp for tumors other than MCC.

### RNA *in situ* hybridization

The RNAscope 2.5 HD BROWN assay (Cat. No. 322300) (Advanced Cell Diagnostics, Hayward, CA) was performed using target probes to MCPyV on TMA slides, according to the manufacturer's instructions. The RNA probes (Hs-V-MCPyV-LT-ST-Ag, accession # NC_010277.1, nucleotides 197-1448) contained 14 pairs of probes (conceptualized as ZZ) complementary to the target mRNA. Probes Hs-PPIB (human peptidylprolyl isomerase B) and DapB (bacterial dihydrodipicolinate reductase) were used as positive and negative controls, respectively. FFPE sections were baked at 60°C for one hour. Tissues were deparaffinized by immersing in xylene twice for five minutes each with periodic agitation. The slides were immersed in 100% ethanol twice for one minute each with periodic agitation and then air-dried for five minutes. After a series of pretreatment steps, the cells were permeabilized using Protease Plus to allow probes access to the RNA target. Hybridization of the probes to the RNA targets was performed by incubation in the HybEZ™ Oven for two hours at 40°C. After two washes, the slides were processed for standard signal amplification steps. Chromogenic detection was performed using DAB followed by counterstaining with 50% Gill's Hematoxylin I (Fisher, 26801-01).

All slides were examined for MCPyV ISH signals in morphologically intact cells and scored independently by two study pathologists (L.W. and P.W.H.) who were blinded to associated qPCR data. MCPyV ISH signal was identified as brown, punctate dots, and expression level was scored as follows: 0 = no staining or less than 1 dot per 10 cells, 1 =1 to 3 dots per cell, 2 =4 to 9 dots per cell (few or no dot clusters), 3 =10 to 15 dots per cell (less than 10% in dot clusters), and 4 = greater than 15 dots per cell (more than 10% in dot clusters) (21). Representative photomicrographs of samples showing different MCPyV RNA-ISH intensities are illustrated in Supplementary Figure S1. As previously described, a cumulative ISH product score was calculated for each evaluable tissue core as the sum of the individual products of the expression level (0 to 4) and percentage of cells (0 to 100) (i.e., [A%× 0] + [B%× 1] +[C%× 2] + [D% × 3] + [E% × 4]; total range =0 to 400) (22). For each tissue sample, the ISH product score was averaged across evaluable TMA tissue cores. In this study, tumors that were considered positive had scores greater than or equal to 5, and tumors with product scores of 0 were considered negative.

### DNA extraction and quantitative PCR

Two 10 μm tissue sections per specimen were used, with macrodissection in some cases to maximize tumor purity. 30 tumors lacked sufficient remaining material or otherwise were unavailable for MCPyV qPCR detection. FFPE tumor was deparaffinized and DNA was extracted using the QIAamp DSP DNA FFPE Tissue Kit, following the manufacturer's instructions. DNA quantification was performed by Qubit 3.0 Fluorometer (Invitrogen, Carlsbad, CA) and diluted if necessary. 15 ng input DNA was analyzed by qPCR on the StepOne real-time PCR system (Applied Biosystems, Foster City, CA) using Taqman detection with the previously reported LT2 (LTAg) primer/probe set and SET9 (sTAg) primer/probe set (14). RNaseP TaqMan copy number reference assay (Thermo Fisher Scientific, Waltham, MA) was used to normalize results and confirm adequacy of DNA for PCR. All samples were run in triplicate. The MKL-2 cell line was used as the standard for one viral copy/cell genome, as previously described (6, 14). Negative controls included purified, distilled water and DNA from HEK 293 (human embryonic kidney 293) cells.

### Statistical analysis

The experimental data were expressed as the mean ± standard deviation, and the statistical significance between different groups was determined using t-tests. The relationship between MCPyV transcript expression and clinicopathological features of MCC patients was analyzed using $\chi^2$ and Fisher's exact tests. Statistical significance was defined as a *P*-value less than 0.05.

## Results

### Clinical characteristics of the cohort

87 different tumor tissues from 75 MCC patients were included in the study. The median age of the MCC patients tested was 73 years (range 48–89 years), and 64% (n=48) were male and 36% (n=27) were female. These included 25 primary tumors and 62 metastatic tumors. Eight patients with matched primary-metastasis pairs were tested. Of the 75 patients, four

patients had two metastatic tumors. Lymph nodes were the most common metastatic sites. Clinicopathological characteristics of this cohort are described in Table 1.

### Nomination of RNA-ISH probe target region

To determine regions of MCPyV transcript in highest abundance in MCC, we evaluated previously collected RNAseq data from MCPyV-positive tumors (6). The most consistently detected region was at the 5′ end of LTAg exon 2 (also shared by ALTO and 57kT transcripts) (Supplementary Figure S2) (3, 23, 24), overlapping with a commonly targeted region for qPCR detection of MCPyV (Figure 1). However, we and others have observed cases with high sTAg and low LTAg expression by qPCR (14, 25). Therefore, a probe encompassing nucleotides 197-1448 (both sTAg and LTAg regions) was selected (Figure 1).

### MCPyV RNA-ISH assay specifically detects the presence of MCPyV in MCC samples

To demonstrate the feasibility of the RNAscope MCPyV-assay, we first performed *in situ* hybridization with the selected probe on three MCCs previously shown to harbor MCPyV by qPCR. MCPyV RNA-ISH revealed brown, punctate dots mainly located in the nuclei with no background expression, whereas the negative control probe (DapB) demonstrated no expression (Figure 2). In contrast, no punctate dots were detected in diverse tissues, including three cases of MCPyV-negative MCCs (previously confirmed to be negative by qPCR), nine cases of cervical carcinoma, four cases of non-cutaneous small cell carcinoma, one case of basal cell carcinoma, six benign cervix tissues, and two normal skin tissues.

### MCPyV RNA-ISH identifies associations of age and gender with MCPyV positivity

RNAscope MCPyV test was carried out on MCC TMAs and whole tissue sections totaling 93 different tumor samples. Six cases had insufficient staining for the positive control (PPIB) and were hence excluded from further analysis, leaving 87/93 (93.5%) samples for MCPyV RNA-ISH analysis. Of these 75 patients, 37 (49.3%) cases were positive for MCPyV RNA-ISH, with corroboration by qPCR in a subset of cases as described further below (examples of staining, Figure 3). Of the 25 primary tumors, nine (36%) cases were positive for MCPyV (mean ISH product score = 95; range = 25 to 320). Of the 62 metastatic tumors, 33 (53.2%) cases were positive for MCPyV (mean ISH product score = 140; range = 5 to 225). The percentage of positive cells in MCPyV-positive cases ranged from 5% to 100% (Supplementary Figure S3A). Of the eight matched primary-metastatic pairs, five pairs were negative and three pairs were positive. There was no significant difference in MCPyV expression between primary and metastatic tumors. Samples derived from the same patient were concordant in terms of MCPyV status.

Table 1 summarizes the correlation of MCPyV status detected by RNA-ISH with clinicopathological features. There were 37 patients younger than 73 years and 38 patients older than 73. Notably, tumors from younger patients (< 73 years) had a significantly higher virus positivity rate than those from the elderly (≥ 73 years) (64.9% vs. 34.2%, $P$=0.011) (Figure 4A). Furthermore, tumors from female patients had a higher positive rate of MCPyV than those from male patients (66.7% vs. 39.6%, $P$=0.032) (Figure 4B). There was no relationship between MCPyV status and tumor site.

We also evaluated agreement between TMA cores from a given case and between TMA cores and matched whole tissue sections. RNA-ISH demonstrated marked agreement/concordance among multiple TMA cores for a given case (98.5% agreement across 66 cases) and between TMA cores and matched whole tissue sections (100% agreement across six cases).

### MCPyV qPCR of MCC samples and comparison with RNA-ISH detection

To assess the utility of RNA-ISH compared to qPCR for detection of MCPyV, we evaluated 57 tumor samples from 52 cases of our MCC cohort by qPCR of tumor DNA for the presence of MCPyV LTAg (LT2) and sTAg (SET9) sequence. Of the 52 patients, four patients had two metastatic tumors, and one patient had a matched primary-metastasis pair. The detection rates of MCPyV by LT2 and SET9 primer/probe sets were 55.8% (29/52) and 53.8% (28/52), respectively. One sample (MCC/25, Patient 12) with low tumor content was positive by LT2 (0.004 estimated copies per genome) but negative by SET9; the presence of viral transcript was confirmed in tumor cells (Supplementary Figure S3B). Therefore, a qPCR copy number of 0.004 by LT2 was the minimal value considered positive for MCPyV (Supplementary Table 1). There was a strong correlation between LTAg and sTAg copy number (Spearman's correlation coefficient $R^2 = 0.971$, $P < 0.0001$) (Figure 4C).

Of the 10 primary tumors, four (40%) cases were positive for MCPyV; virus copy number by LT2 and SET9 ranged from 0.071 to 0.355, and 0.057 to 0.107, respectively. Of the 47 metastatic tumors, 28 (59.6%) cases were positive for MCPyV; virus copy number by LT2 and SET9 ranged from 0.004 to 3.763, and 0.010 to 1.759, respectively. In the single patient with qPCR data for both primary tumor and metastatic tumor, the qPCR values were 0.352 and 0.598 for LT2, and 0.019 and 0.060 for SET9, respectively.

To confirm specificity of qPCR and determine MCPyV levels that might be detected in non-MCC tissues, qPCR was also performed on 18 cases of normal skin and one case of small cell carcinoma of the lung to establish background levels of MCPyV in non-tumor or non-MCC tissues. From these control tissues, only one case of normal skin demonstrated signal for MCPyV (virus copy number by LT2 and SET9 was 0.007 and 0.0007, respectively). MCPyV RNA-ISH was negative in this sample. MCPyV in this case (presumed background infection) exceeded virus copy number in MCC/25 detected by qPCR; however, RNA-ISH was specific for tumor-associated MCPyV in this context.

A total of 57 samples had data from both detection modalities (RNA-ISH and qPCR) for direct comparison, and the results are shown in Figure 4D. Considering MCPyV LTAg qPCR results as the gold standard for determining MCPyV status, the RNAscope test had 100% sensitivity and 100% specificity (Figure 3). There was a strong correlation between qPCR copy number by LT2 and RNA-ISH product score (Spearman's correlation coefficient $R^2 = 0.926$, $P < 0.0001$) (Figure 4D), demonstrating the validity of RNA-ISH as a highly-sensitive assay to detect MCPyV in patient samples. Interestingly, we found that the percentage of tumor cells labeled by RNA-ISH also had a significant correlation with viral copy number (Spearman's correlation coefficient $R^2 = 0.925$, $P < 0.0001$) (Supplementary Figure S3C).

## Discussion

MCPyV is currently the only polyomavirus to be strongly associated with tumors in humans (2). Wild-type MCPyV may reside in skin and other tissues, with a high prevalence of infection in the general population (15, 26, 27). MCPyV-associated MCC is thought to arise in the rare event when MCPyV aberrantly integrates into the genome of the tumor progenitor cell and undergoes truncation or mutation of the LTAg gene that renders the virus replication-deficient but transformation-competent (2). Deregulated viral T antigens then drive tumorigenesis via multiple mechanisms (2).

As MCPyV is commonly present in MCC but not histologic mimics, such as non-cutaneous small cell carcinoma, detection assays for MCPyV are entering clinical use as a diagnostic test for MCC. In addition, the differing genetic drivers and mutational profiles of MCPyV-positive and MCPyV-negative MCC may have translational significance for prognosis and therapeutics, suggesting further rationale for characterization of MCPyV status (4–6). Although reports on prognostic significance have been mixed regarding whether the presence of MCPyV detection is associated with improved outcome, a recent large prospective study of 282 cases using multimodal MCPyV detection with qPCR and IHC demonstrated significantly better outcome for MCPyV-positive tumors (28). In addition, the presence of MCPyV may influence tumor sensitivity to immunotherapy and targeted therapy (5, 29, 30). Hence, detection of MCPyV in MCC tumors has diagnostic and prognostic utility and may have a future role in guiding management.

Here, we show that RNA-ISH represents a novel and effective method for detection of MCPyV in MCC tumors. As predicted, RNA-ISH was highly specific for MCC and matched qPCR in sensitivity. Unlike IHC and conventional qPCR, RNA-ISH allows for simultaneous detection of sTAg and LTAg in a single assay. There was substantial agreement among TMA cores and whole tissue sections for RNA-ISH; although the number of comparisons with whole tissue sections was relatively small, our findings suggest that RNA-ISH may be reliable in limited samples. Block/tissue age did not appear to represent a technical limitation, as there was no significant difference in block age between positive and negative cases, and the two oldest cases in our cohort (collected 17 and 18 years prior to this study) demonstrated positive staining. Of note, ISH product scores showed a strong correlation with MCPyV copy number estimates by qPCR. This observation indicated a strong association between the number of integrated viral genomes and abundance of T-antigen transcript and correlated with a previous report associating LTAg protein expression with viral copy abundance in MCC (31). Furthermore, we observed a significant correlation between MCPyV copy number by qPCR and the fraction of cells expressing viral transcripts by RNA-ISH, a finding that could be explained by loss of integrated MCPyV in a fraction of tumor cells (14).

RNA-ISH detection of MCPyV compares favorably with established methods of MCC detection (Table 2). Because MCPyV is a DNA virus and genomically integrated in the setting of MCC tumors, qPCR is highly sensitive for the presence of MCPyV in tumor genomes. By qPCR, there is extreme variability in the number of integrated viral genomes that may be detected in MCC tumors, and some have proposed that differences in copy

burden may be biologically significant (14, 31). Although highly sensitive and quantitative, qPCR has several limitations in this context. Some tumors may lack detectable LTAg or sTAg; therefore, multiple amplicons must be evaluated for maximal sensitivity (14). In addition, qPCR does not allow for direct correlation with tissue morphology, hence preventing confirmation of adequate tumor content and localization of signal to tumor cells. This is relevant because qPCR may detect the presence of wild-type MCPyV in various tissues (27), and reliable cutoffs have not been demonstrated for distinguishing background MCPyV infection from tumor MCPyV. Hence, there is potential for false positive results by qPCR. In our cohort, one tumor (MCC/25, Patient 12) had very low copy number by qPCR (likely due to low tumor content) that could not have been distinguished from nonspecific signal we observed in normal skin by qPCR. However, RNA-ISH was able to demonstrate MCPyV transcript in tumor cells in this sample. Furthermore, based upon comparison with analogous clinical assays at our institution, we estimate that costs for RNA-ISH will be equivalent to or less than for qPCR. Together, RNA-ISH represents a highly sensitive and cost-effective alternative to qPCR, with superior precision in the setting of challenging samples with low tumor purity or low MCPyV copy number. RNA-ISH enables rapid, accurate assessment of MCPyV transcripts in FFPE clinical tissue samples at unprecedented levels of consistency and reproducibility without the need for lengthy rounds of assay optimization (18).

IHC for viral T antigens is an alternative method for MCPyV detection. The most commonly utilized antibody is the commercially-available clone CM2B4, which detects MCPyV LTAg with high specificity. However, CM2B4 has been shown to have limited sensitivity relative to qPCR (14, 31). Other methods that have also been reported in the literature include fluorescence *in situ* hybridization (FISH) and IsHyb ISH (32–34). However, the interpretation/reporting of FISH results can be challenging. Matsushita *et al.* (34) demonstrated the feasibility of IsHyb ISH for MCPyV sTAg mRNA but found this to be incompletely sensitive in comparison to qPCR, in contrast to our RNA-ISH approach targeting both large and small T antigen transcripts.

In this study, the median age of the MCC patients tested was 73 years. Tumors from younger patients (< 73 years) had significantly higher virus positivity rates than those from the elderly (≥ 73 years) (64.9% vs. 34.2%, $P$ =0.011). Hence, older patients seemed more likely to develop MCC by exposure to ultraviolet (UV) radiation from the sun rather than MCPyV integration. Another significant difference in our cohort was the higher proportion of MCPyV-positive tumors in female patients. Schrama *et al.* (35) also reported that MCPyV-positive cases were significantly more likely to be in female patients. Men have an overall higher incidence of skin cancer than women (36), in agreement with the observation of relatively higher incidence of MCPyV-negative (UV-associated) MCC in men. More extensive studies are needed to confirm these associations with MCPyV status; however, these and other epidemiologic factors may explain why our rate of detected MCPyV across both modalities is slightly lower than often reported. Our assays were conducted with appropriate controls, and our rate of MCPyV positivity is similar to previous reports from our institution with a variety of detection approaches (6, 37–39), suggesting that our lower rate of MCPyV positivity in this study is related to the patient cohort rather than technical factors.

In summary, we demonstrate that RNA-ISH is a sensitive and specific assay for MCPyV detection in MCC that is comparable to qPCR in sensitivity but has the additional benefit of allowing for correlation with tissue findings. We find that qPCR does not reliably distinguish low tumor content from nonspecific background signal, whereas RNA-ISH confirms viral transcript expression in tumor cells in such cases. RNA-ISH also provides quantitative data on MCPyV transcript expression that directly correlates with viral copy number burden. These findings support RNA-ISH as an effective method for MCPyV detection in tumors that could be implemented in clinical practice. Furthermore, our study reveals a significant association between patient age, gender, and MCPyV positivity such that MCPyV was more frequently present in female or younger (<73 years old) MCC patients. Our results suggest that male or older (≥73 years old) MCC patients may require more careful monitoring for recurrence and metastasis than their respective counterparts.

## Supplementary Material

Refer to Web version on PubMed Central for supplementary material.

## Acknowledgments

The authors would like to thank Brendan A. Veeneman for help with figures; Stephanie Ellison for manuscript editing; and Karen Giles for assistance with manuscript submission.

**Financial Support:** P.W. Harms was supported by the Dermatopathology Research Career Development Award from the Dermatology Foundation.

## References

1. Erstad DJ, J C Jr. Mutational analysis of merkel cell carcinoma. Cancers (Basel). 2014; 6:2116–36. [PubMed: 25329450]
2. Bhatia S, Afanasiev O, Nghiem P. Immunobiology of Merkel cell carcinoma: implications for immunotherapy of a polyomavirus-associated cancer. Curr Oncol Rep. 2011; 13:488–97. [PubMed: 21953511]
3. Feng H, Shuda M, Chang Y, Moore PS. Clonal integration of a polyomavirus in human Merkel cell carcinoma. Science. 2008; 319:1096–100. [PubMed: 18202256]
4. Wong SQ, Waldeck K, Vergara IA, Schroder J, Madore J, Wilmott JS, et al. UV-associated mutations underlie the etiology of MCV-negative Merkel cell carcinomas. Cancer Res. 2015; 75:5228–34. [PubMed: 26627015]
5. Goh G, Walradt T, Markarov V, Blom A, Riaz N, Doumani R, et al. Mutational landscape of MCPyV-positive and MCPyV-negative Merkel cell carcinomas with implications for immunotherapy. Oncotarget. 2016; 7:3403–15. [PubMed: 26655088]
6. Harms PW, Vats P, Verhaegen ME, Robinson DR, Wu YM, Dhanasekaran SM, et al. The distinctive mutational spectra of polyomavirus-negative Merkel cell carcinoma. Cancer Res. 2015; 75:3720–7. [PubMed: 26238782]
7. Cimino PJ, Robirds DH, Tripp SR, Pfeifer JD, Abel HJ, Duncavage EJ. Retinoblastoma gene mutations detected by whole exome sequencing of Merkel cell carcinoma. Mod Pathol. 2014; 27:1073–87. [PubMed: 24406863]
8. Garneski KM, Warcola AH, Feng Q, Kiviat NB, Leonard JH, Nghiem P. Merkel cell polyomavirus is more frequently present in North American than Australian Merkel cell carcinoma tumors. J Invest Dermatol. 2009; 129:246–8. [PubMed: 18650846]
9. Mertz KD, Paasinen A, Arnold A, Baumann M, Offner F, Willi N, et al. Merkel cell polyomavirus large T antigen is detected in rare cases of nonmelanoma skin cancer. J Cutan Pathol. 2013; 40:543–9. [PubMed: 23521575]

10. Ly TY, Walsh NM, Pasternak S. The spectrum of Merkel cell polyomavirus expression in Merkel cell carcinoma, in a variety of cutaneous neoplasms, and in neuroendocrine carcinomas from different anatomical sites. Hum Pathol. 2012; 43:557–66. [PubMed: 21940035]
11. Jung HS, Choi YL, Choi JS, Roh JH, Pyon JK, Woo KJ, et al. Detection of Merkel cell polyomavirus in Merkel cell carcinomas and small cell carcinomas by PCR and immunohistochemistry. Histol Histopathol. 2011; 26:1231–41. [PubMed: 21870327]
12. Paik JY, Hall G, Clarkson A, Lee L, Toon C, Colebatch A, et al. Immunohistochemistry for Merkel cell polyomavirus is highly specific but not sensitive for the diagnosis of Merkel cell carcinoma in the Australian population. Hum Pathol. 2011; 42:1385–90. [PubMed: 21453956]
13. Busam KJ, Jungbluth AA, Rekthman N, Coit D, Pulitzer M, Bini J, et al. Merkel cell polyomavirus expression in merkel cell carcinomas and its absence in combined tumors and pulmonary neuroendocrine carcinomas. Am J Surg Pathol. 2009; 33:1378–85. [PubMed: 19609205]
14. Rodig SJ, Cheng J, Wardzala J, DoRosario A, Scanlon JJ, Laga AC, et al. Improved detection suggests all Merkel cell carcinomas harbor Merkel polyomavirus. J Clin Invest. 2012; 122:4645–53. [PubMed: 23114601]
15. Schowalter RM, Pastrana DV, Pumphrey KA, Moyer AL, Buck CB. Merkel cell polyomavirus and two previously unknown polyomaviruses are chronically shed from human skin. Cell Host Microbe. 2010; 7:509–15. [PubMed: 20542254]
16. Leroux-Kozal V, Leveque N, Brodard V, Lesage C, Dudez O, Makeieff M, et al. Merkel cell carcinoma: histopathologic and prognostic features according to the immunohistochemical expression of Merkel cell polyomavirus large T antigen correlated with viral load. Hum Pathol. 2015; 46:443–53. [PubMed: 25623078]
17. Hattori T, Takeuchi Y, Takenouchi T, Hirofuji A, Tsuchida T, Kabumoto T, et al. The prevalence of Merkel cell polyomavirus in Japanese patients with Merkel cell carcinoma. J Dermatol Sci. 2013; 70:99–107. [PubMed: 23517683]
18. Wang F, Flanagan J, Su N, Wang LC, Bui S, Nielson A, et al. RNAscope: a novel in situ RNA analysis platform for formalin-fixed, paraffin-embedded tissues. J Mol Diagn. 2012; 14:22–9. [PubMed: 22166544]
19. Shi J, Liu H, Ma XJ, Chen Z, He MX, Luo Y, et al. Ribonucleic acid in situ hybridization is a more sensitive method than immunohistochemistry in detection of thyroid transcription factor 1 and Napsin A expression in lung adenocarcinomas. Arch Pathol Lab Med. 2016; 140:332–40. [PubMed: 27028392]
20. Anderson CM, Zhang B, Miller M, Butko E, Wu X, Laver T, et al. Fully automated RNAscope in situ hybridization assays for formalin-fixed paraffin-embedded cells and tissues. J Cell Biochem. 2016; 117:2201–8. [PubMed: 27191821]
21. Warrick JI, Tomlins SA, Carskadon SL, Young AM, Siddiqui J, Wei JT, et al. Evaluation of tissue PCA3 expression in prostate cancer by RNA in situ hybridization–a correlative study with urine PCA3 and TMPRSS2-ERG. Mod Pathol. 2014; 27:609–20. [PubMed: 24072184]
22. Mehra R, Udager AM, Ahearn TU, Cao X, Feng FY, Loda M, et al. Overexpression of the long non-coding RNA SChLAP1 independently predicts lethal prostate cancer. Eur Urol. 2016; 70:549–552. [PubMed: 26724257]
23. Carter JJ, Daugherty MD, Qi X, Bheda-Malge A, Wipf GC, Robinson K, et al. Identification of an overprinting gene in Merkel cell polyomavirus provides evolutionary insight into the birth of viral genes. Proc Natl Acad Sci U S A. 2013; 110:12744–9. [PubMed: 23847207]
24. Shuda M, Arora R, Kwun HJ, Feng H, Sarid R, Fernandez-Figueras MT, et al. Human Merkel cell polyomavirus infection I. MCV T antigen expression in Merkel cell carcinoma, lymphoid tissues and lymphoid tumors. Int J Cancer. 2009; 125:1243–9. [PubMed: 19499546]
25. Shuda M, Kwun HJ, Feng H, Chang Y, Moore PS. Human Merkel cell polyomavirus small T antigen is an oncoprotein targeting the 4E-BP1 translation regulator. J Clin Invest. 2011; 121:3623–34. [PubMed: 21841310]
26. Tolstov YL, Pastrana DV, Feng H, Becker JC, Jenkins FJ, Moschos S, et al. Human Merkel cell polyomavirus infection II. MCV is a common human infection that can be detected by conformational capsid epitope immunoassays. Int J Cancer. 2009; 125:1250–6. [PubMed: 19499548]

27. Matsushita M, Kuwamoto S, Iwasaki T, Higaki-Mori H, Yashima S, Kato M, et al. Detection of Merkel cell polyomavirus in the human tissues from 41 Japanese autopsy cases using polymerase chain reaction. Intervirology. 2013; 56:1–5. [PubMed: 22986833]

28. Moshiri AS, Doumani R, Yelistratova L, Blom A, Lachance K, Shinohara MM, et al. Polyomavirus-Negative Merkel Cell Carcinoma: A more aggressive subtype based on analysis of 282 cases using multimodal tumor virus detection. J Invest Dermatol. 2017; 137:819–827. [PubMed: 27815175]

29. Nghiem PT, Bhatia S, Lipson EJ, Kudchadkar RR, Miller NJ, Annamalai L, et al. PD-1 blockade with pembrolizumab in advanced Merkel-cell carcinoma. N Engl J Med. 2016; 374:2542–52. [PubMed: 27093365]

30. Arora R, Shuda M, Guastafierro A, Feng H, Toptan T, Tolstov Y, et al. Survivin is a therapeutic target in Merkel cell carcinoma. Sci Transl Med. 2012; 4:133ra56.

31. Bhatia K, Goedert JJ, Modali R, Preiss L, Ayers LW. Immunological detection of viral large T antigen identifies a subset of Merkel cell carcinoma tumors with higher viral abundance and better clinical outcome. Int J Cancer. 2010; 127:1493–6. [PubMed: 20041469]

32. Haugg AM, Rennspiess D, zur Hausen A, Speel EJ, Cathomas G, Becker JC, et al. Fluorescence in situ hybridization and qPCR to detect Merkel cell polyomavirus physical status and load in Merkel cell carcinomas. Int J Cancer. 2014; 135:2804–15. [PubMed: 24771111]

33. Haugg AM, Speel EJ, Pantulu ND, Pallasch C, Kurz AK, Kvasnicka HM, et al. Fluorescence in situ hybridization confirms the presence of Merkel cell polyomavirus in chronic lymphocytic leukemia cells. Blood. 2011; 117:5776–7. [PubMed: 21617011]

34. Matsushita M, Nonaka D, Iwasaki T, Kuwamoto S, Murakami I, Kato M, et al. A new in situ hybridization and immunohistochemistry with a novel antibody to detect small T-antigen expressions of Merkel cell polyomavirus (MCPyV). Diagn Pathol. 2014; 9:65. [PubMed: 24649978]

35. Schrama D, Peitsch WK, Zapatka M, Kneitz H, Houben R, Eib S, et al. Merkel cell polyomavirus status is not associated with clinical course of Merkel cell carcinoma. J Invest Dermatol. 2011; 131:1631–8. [PubMed: 21562568]

36. Force USPST. Bibbins-Domingo K, Grossman DC, Curry SJ, Davidson KW, Ebell M, et al. Screening for skin cancer: US preventive services task force recommendation statement. JAMA. 2016; 316:429–35. [PubMed: 27458948]

37. Harms PW, Patel RM, Verhaegen ME, Giordano TJ, Nash KT, Johnson CN, et al. Distinct gene expression profiles of viral- and nonviral-associated merkel cell carcinoma revealed by transcriptome analysis. J Invest Dermatol. 2013; 133:936–45. [PubMed: 23223137]

38. Verhaegen ME, Mangelberger D, Weick JW, Vozheiko TD, Harms PW, Nash KT, et al. Merkel cell carcinoma dependence on bcl-2 family members for survival. J Invest Dermatol. 2014; 134:2241–50. [PubMed: 24614157]

39. Andea AA, Patel R, Ponnazhagan S, Isayeva T, Kumar S, Siegal GP. Detection of Merkel cell polyomavirus in formalin-fixed, paraffin-embedded tissue of Merkel cell carcinoma and correlation with prognosis. Rom J Morphol Embryol. 2014; 55:1057–62. [PubMed: 25607385]

## Statement of Translational Relevance

Merkel cell carcinoma (MCC) is a highly aggressive neuroendocrine tumor of the skin. Merkel cell polyomavirus (MCPyV) plays an oncogenic role in most cases of MCC. Detection of MCPyV has diagnostic utility in distinguishing MCC from histologically-similar tumors and also has potential prognostic and therapeutic implications. Existing MCPyV assays, quantitative PCR (qPCR) and immunohistochemistry (IHC), have limitations for routine clinical practice or can be non-specific. We evaluated RNA *in situ* hybridization (RNA-ISH) as a modality for MCPyV detection in 87 MCC tumors. We demonstrated that RNA-ISH was comparably sensitive and specific to qPCR for the detection of MCPyV and allowed for correlation with tissue morphology to evaluate for low tumor content and background non-tumor infection by MCPyV. Importantly, this study also reveals a significant association between patient age, gender, and MCPyV positivity.

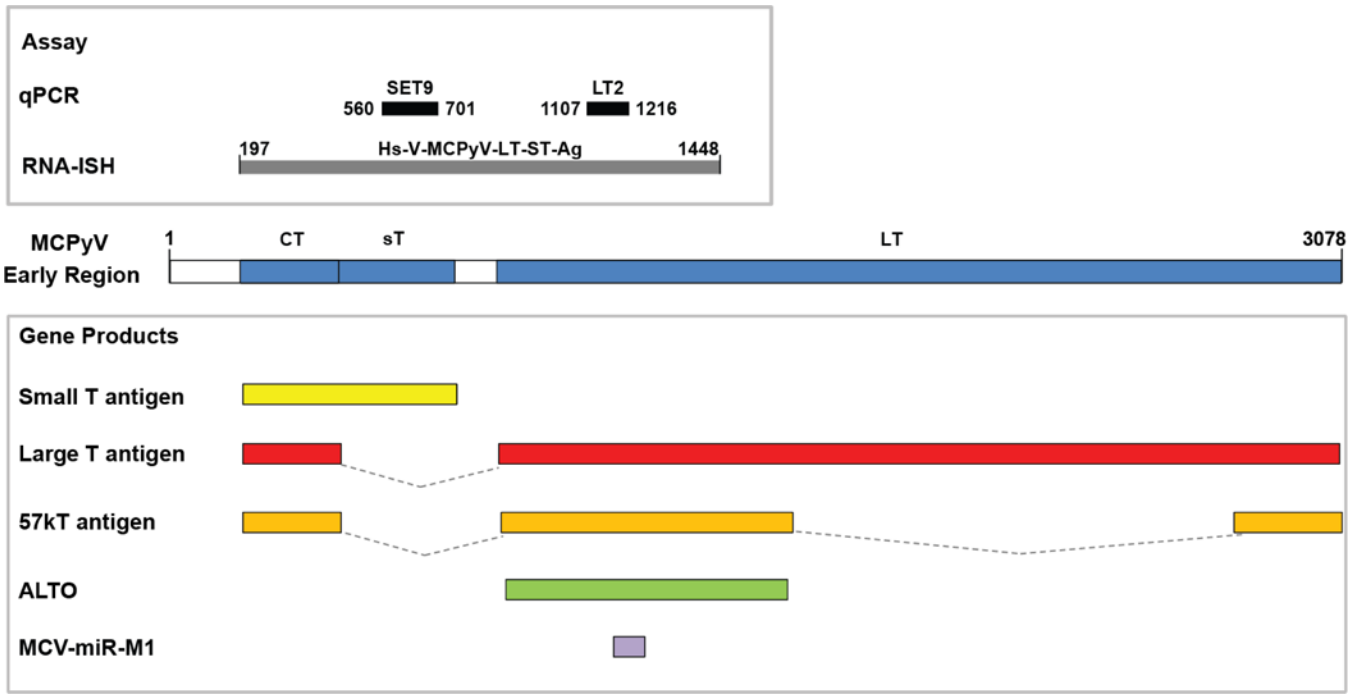


**Figure 1.**

Schematic of MCPyV early region, including location of T-antigen transcripts and other proposed transcripts (bottom). Regions targeted by MCPyV detection assays used in this study are shown at top. LT2 and SET9 primer/probe sets were designed to amplify sequences corresponding to nucleotides 1107–1216 of MCPyV encoding LTAg, and 560–701 of MCPyV encoding sTAg, respectively. The RNA probe (Hs-V-MCPyV-LT-ST-Ag) was designed to encompass nucleotides 197-1448 (both sTAg and LTAg regions). CT, Common T antigen region; sT, small T antigen unique region; LT, Large T antigen 2$^{nd}$ exon.

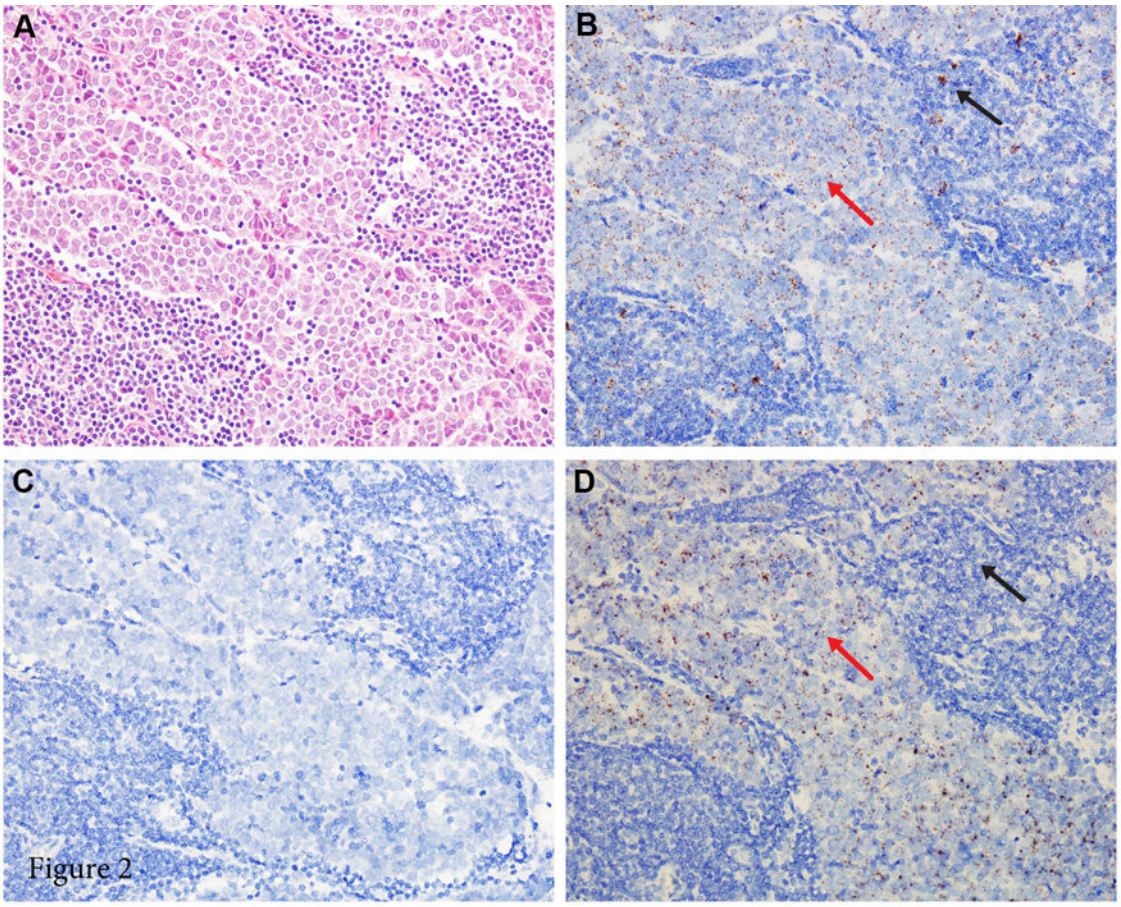


**Figure 2.**

Photomicrographs of a Merkel cell carcinoma with positive MCPyV RNA *in situ* hybridization (RNA-ISH). (A) Histologic features of Merkel cell carcinoma: monotonous tumor cells with round nuclei, finely granular and dusty chromatin, and inconspicuous nucleoli (hematoxylin and eosin, 200× magnification). (B) PPIB staining, used as positive control to confirm that RNA quality is sufficient (200× magnification); both tumor cells (red arrow) and lymphocytes (black arrow) stain positively. (C) DapB staining, used as negative control (200× magnification). (D) Positive MCPyV RNA-ISH with punctate brown staining (200× magnification); tumor cells stain positively (red arrow) and lymphocytes stain negatively (black arrow).

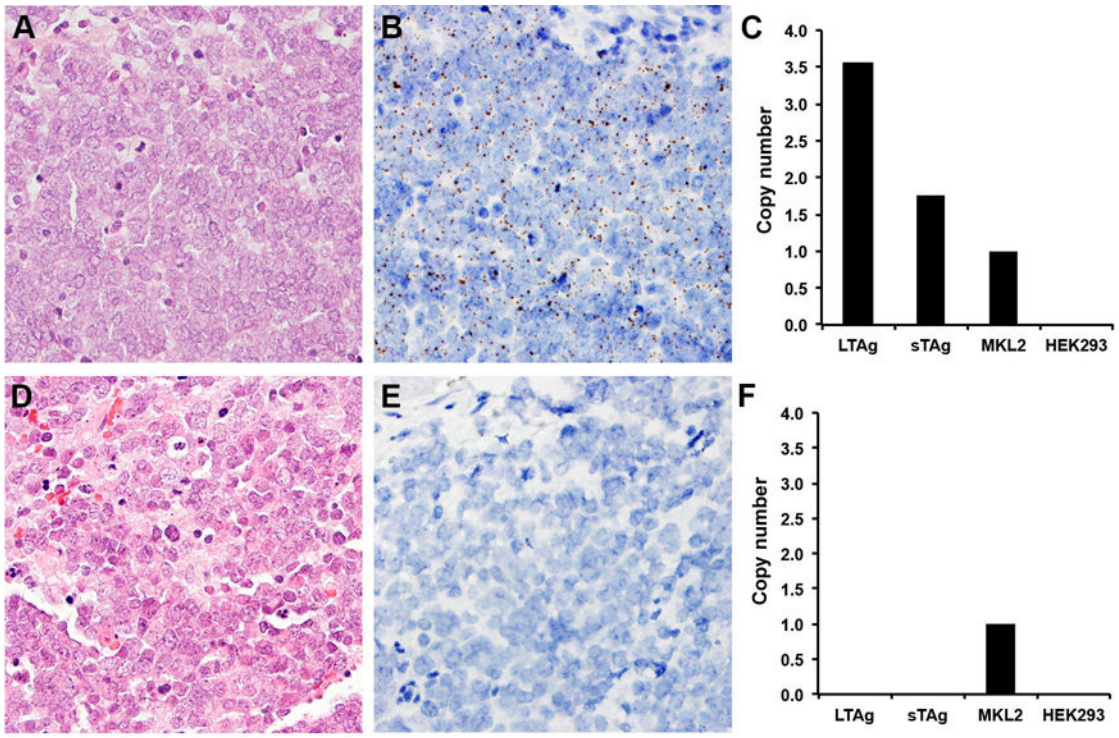


**Figure 3.**

Representative examples of RNA-ISH in comparison to qPCR. (A, D) Merkel cell carcinoma (hematoxylin and eosin, 400× magnification). (B) Representative MCPyV-positive tumor by RNA-ISH. RNA-ISH revealed brown, punctate dots mainly located in the nuclei with no background staining (400× magnification). (C) Corresponding MCPyV copy numbers by LT2 and SET9 primer/probe sets, respectively. The MKL-2 cell line was used as the standard for one viral copy/cell genome. The HEK 293 cell line was used as the negative control. (E) Representative MCPyV-negative tumor by RNA-ISH (400× magnification). (F) Corresponding negative results by qPCR.

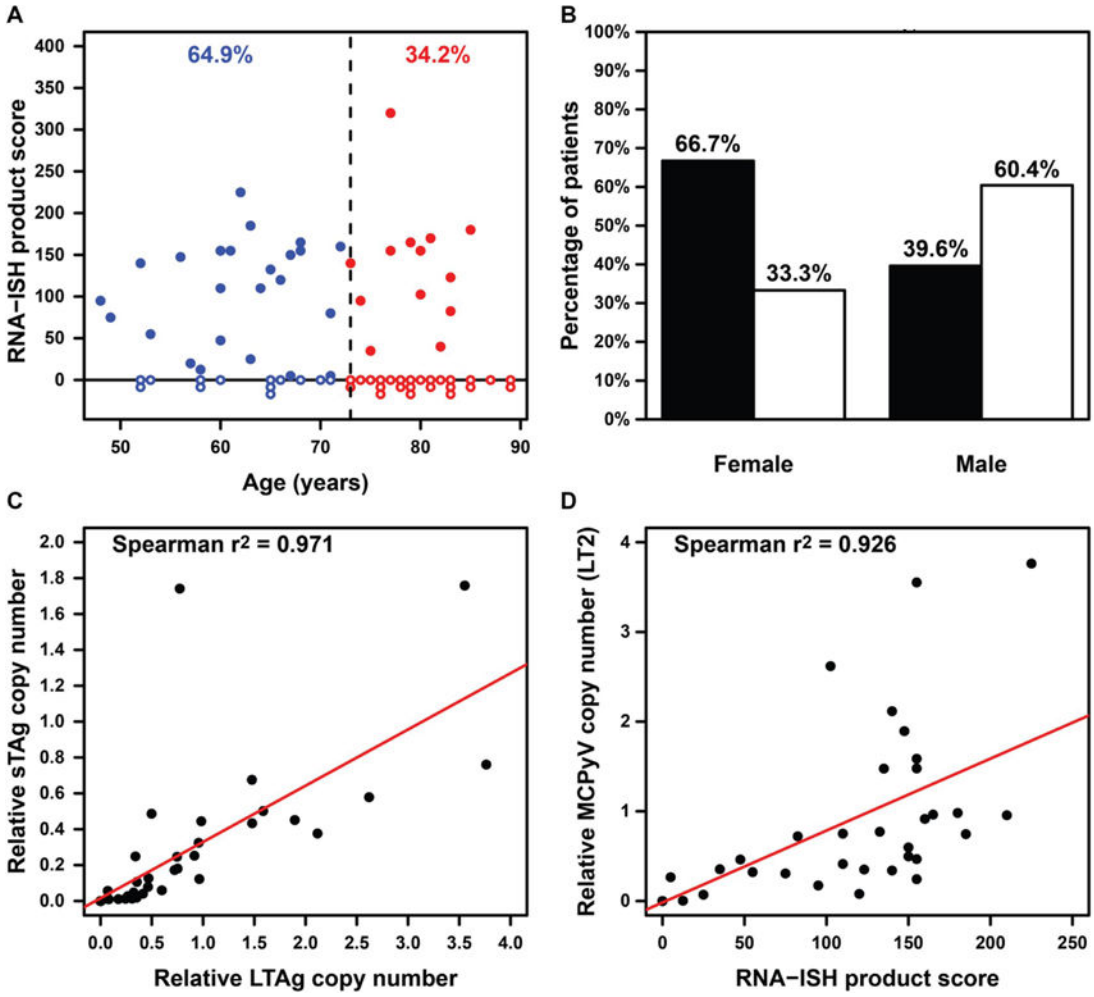


**Figure 4.**

(A) The distribution of MCPyV positive and negative tumors as detected by RNA-ISH, grouped by patient age. Each dot on X axis represents one tumor from a unique patient. Open dot: MCPyV-negative. Closed dot: MCPyV-positive. Blue color: patient age less than 73 years. Red color: patient age greater than or equal to 73 years. (B) The frequency of MCPyV positive (black bars) and negative (white bars) tumors as detected by RNA-ISH, grouped by patient gender. (C) Comparison of LTAg copy number (LT2, X axis) and sTAg copy number (SET9, Y axis) by qPCR. (D) Comparison of RNA-ISH product score and LTAg copy number by qPCR. In Figure C and D, samples at 0/0 were considered negative and are illustrated as a single dot. All other dots (>0) were considered positive.

## Table 1

Correlation of MCPyV with clinicopathologic features for all Merkel cell carcinoma patients (n = 75) and specimens (n = 87)

| Features | N (%) | MCPyV, n (%) | | *P* |
|---|---|---|---|---|
| | | Positive | Negative | |
| Age (n=75) | | | | |
| <73 | 37 (49.3%) | 24 (64.9%) | 13 (25.1%) | **0.011** * |
| ≥73 | 38 (50.7%) | 13 (34.2%) | 25 (65.8%) | |
| Patient sex (n=75) | | | | |
| Male | 48 (64%) | 19 (39.6%) | 29 (60.4%) | **0.032** * |
| Female | 27 (36%) | 18 (66.7%) | 9 (33.3%) | |
| Breslow depth (n=25) | | | | |
| 0–5mm | 10 (40%) | 3 (30%) | 7 (70%) | 0.413 ** |
| 6–10mm | 6 (24%) | 1 (16.7%) | 5 (83%) | |
| >10 mm | 3 (12%) | 2 (66.7%) | 1 (33.3%) | |
| Unknown | 6 (24%) | 3 (50%) | 3 (50%) | |
| Primary tumors (n=25) | | | | |
| Head and neck | 11 (44%) | 3 (27.3%) | 8 (72.7%) | 0.704 ** |
| Extremities | 12 (48%) | 5 (41.7%) | 7 (58.3%) | |
| Trunk | 2 (8%) | 1 (50%) | 1 (50%) | |
| Metastatic tumors (n=62) | | | | |
| Local recurrence [a] | 3 (4.8%) | 1 (33.3%) | 2 (66.7%) | 0.722 ** |
| Satellite/in transit | 13 (21.0%) | 8 (61.5%) | 5 (38.5%) | |
| Lymph nodes | 40 (64.5%) | 21 (52.5%) | 19 (47.5%) | |
| Parotid | 5 (8.0%) | 2 (40%) | 3 (60%) | |
| Unknown | 1 (1.6%) | 1(100%) | 0 (0%) | |

* Fisher's exact test was used;

** $\chi^2$ test was used;

[a] Locally recurrent tumors were included in the metastatic tumor group for this analysis.

MCPyV, Merkel cell polyomavirus.

**Table 2**

Advantages and limitations of currently available Merkel cell polyomavirus detection methods

| Detection technique | Advantages | Limitations |
|---|---|---|
| Quantitative PCR<br>or<br>Reverse transcription PCR | High sensitivity<br>Feasible on FFPE material<br>Quantitative | Requires DNA/RNA extraction<br>Possibility of false-positive<br>Multiple primer sets are needed<br>Risk of RNA degradation |
| Southern blot | Measurements expressed in absolute values (kb)<br>Feasible on FFPE material<br>May allow for demonstration of genomic integration | Requires DNA extraction<br>Possibility of false-positive<br>Greater quantity of DNA required |
| RNA-ISH | High sensitivity and specificity<br>Feasible on FFPE material<br>Ease of interpretation<br>Correlation with tissue morphology | Semi-quantitative<br>Risk of RNA degradation |
| MCPyV immunostaining | Feasible on FFPE material<br>Correlation with tissue morphology | Reduced sensitivity<br>Possible background staining or weak tumor staining<br>Semi-quantitative |

MCPyV: Merkel cell polyomavirus; RNA-ISH, RNA *in situ* hybridization.